JOURNAL OF GUIDANCE, CONTROL, AND DYNAMICS
Vol. 33, No. 1, January–February 2010

Engineering Notes

Impact Angle Constrained Guidance Against Nonstationary Nonmaneuvering Targets

Ashwini Ratnoo* and Debasish Ghose†
Indian Institute of Science, Bangalore 560 012, India

DOI: 10.2514/1.45026

I. Introduction

GUIDANCE laws with terminal impact angle constraints are widely reported in the literature [1–7]. Proportional navigation guidance (PNG) has been used for deriving impact angle constrained guidance laws for stationary and moving targets. Lu et al. [8] have used PNG in an adaptive guidance law for a hypervelocity impact angle constrained hit at a stationary target. Satisfying impact angle constraint by varying the navigation constant N of the PNG is addressed by Ratnoo and Ghose [9]. In their work [9], a two-stage PNG law is proposed for achieving all impact angles against stationary targets in surface-to-surface engagements. A biased PNG (BPNG) law proposed by Kim et al. [3] has an extra term for annulling the terminal impact angle error together with the conventional line-of-sight rate term for the lateral acceleration command. BPNG law expands the capture region of existing guidance laws against moving targets. However, the performance of BPNG law deteriorates with tail-chase kinds of engagements.

The problem of achieving all impact angles against moving targets is addressed here. The idea of a two-stage PNG law, proposed by Ratnoo and Ghose [9], is further investigated and developed for nonstationary nonmaneuvering targets. It should be noted that for different values of N, the PNG law results in a set of impact angles against a moving target. However, studies on classical PNG law [10] reveal that the value of N should be greater than a minimum value for the terminal lateral acceleration demand to be bounded. The achievable set of impact angles is derived for PNG law, with the values of N satisfying the previously mentioned constraint. To achieve the remaining impact angles, an orientation guidance scheme is proposed for the initial phase of the interceptor trajectory. The orientation guidance law is also PNG law, with N being a function of the initial engagement geometry. It is proven that, following the orientation trajectory, the interceptor can switch to $N = 3$ and achieve any desired impact angle in a surface-to-surface engagement scenario.

II. Impact Angles Against a Nonstationary Nonmaneuvering Target with Proportional Navigation

Consider a planar engagement scenario, shown in Fig. 1a. The target and the interceptor are constant speed point masses moving in a plane. The target is assumed to be nonmaneuvering, and the guidance objective is to intercept the target along a desired impact angle (denoted as α_{mf}). Here, α_m, α_t and θ are the interceptor heading, the target heading, and the line-of-sight angle, respectively. PNG law is defined as

$$\dot{\alpha}_m = N\dot{\theta} \tag{1}$$

Integrating Eq. (1), we get

$$\frac{\alpha_{mf} - \alpha_{m0}}{\theta_f - \theta_0} = N \tag{2}$$

where θ_f is the line-of-sight angle at the time of interception. For interception, the target and the interceptor velocity components normal to the line-of-sight should be equal; that is,

$$v_m \sin(\alpha_{mf} - \theta_f) = v_t \sin(\alpha_t - \theta_f) \tag{3}$$

$$\Rightarrow \theta_f = \tan^{-1}\left[\frac{\sin\alpha_{mf} - \beta\sin\alpha_t}{\cos\alpha_{mf} - \beta\cos\alpha_t}\right] \tag{4}$$

where, β is the target to the interceptor velocity ratio (defined as $\beta = \frac{v_t}{v_m}$). Using Eqs. (2) and (4), we have

$$N = (\alpha_{mf} - \alpha_{m0})/\left(\tan^{-1}\left[\frac{\sin\alpha_{mf} - \beta\sin\alpha_t}{\cos\alpha_{mf} - \beta\cos\alpha_t}\right] - \theta_0\right) \tag{5}$$

Equation (5) relates the desired impact angle α_{mf} to the navigation constant N. The sufficient condition [10] on N for the terminal line-of-sight rate, and hence the terminal lateral acceleration demand to be bounded, is given as

$$N \geq 2(1 + \beta) \tag{6}$$

The targets moving on the surface are slower than the interceptor, and we assume $\beta \leq \frac{1}{2}$ in our domain of interest. Using Eq. (6) with $\beta \leq \frac{1}{2}$, we have

$$N \geq 3 \tag{7}$$

Equation (7) limits the available set of N for achieving different impact angles. With this bound on N, we now determine the set of impact angles that can be achieved by the PNG law. Equation (5) can be rewritten, assuming the ground as the frame of reference with $\alpha_t = 0$, as

$$\frac{\sin\alpha_{mf}}{\cos\alpha_{mf} - \beta} = \tan\left(\frac{\alpha_{mf} - \alpha_{m0}}{N} + \theta_0\right) \tag{8}$$

Solving Eq. (8) for α_{mf} as $N \to \infty$, we have

$$\alpha_{mf} = \theta_0 + \sin^{-1}(-\beta\sin\theta_0) \tag{9}$$

which is the collision heading at $t = 0$. With $N \to \infty$, the interceptor instantaneously attains the collision course. Simplifying Eq. (8) with $N = 3$, we have

$$\frac{\sin\alpha_{mf}}{\cos\alpha_{mf} - \beta} = \tan\left(\frac{\alpha_{mf} - \alpha_{m0}}{3} + \theta_0\right) \tag{10}$$

Let $\alpha_{mf} = \alpha^*_{mf}$ be the solution of Eq. (10); then, the limiting impact angles using PN guidance are given as

$$\alpha_{mf} = \begin{cases} \alpha^*_{mf} & \text{if } N = 3 \\ \theta_0 + \sin^{-1}(-\beta\sin\theta_0) & \text{if } N \to \infty \end{cases} \tag{11}$$

that is,

Received 18 April 2009; revision received 12 September 2009; accepted for publication 17 September 2009.

*Graduate Student, Department of Aerospace Engineering; jmk@aero.iisc.ernet.in.

†Professor, Department of Aerospace Engineering; dghose@aero.iisc.ernet.in.

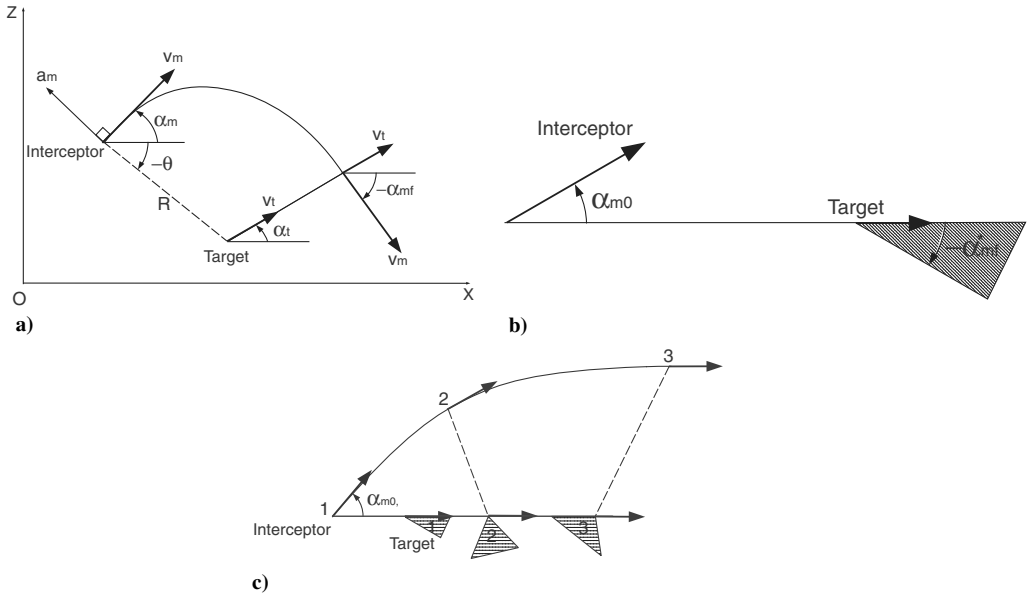

Fig. 1 Engagement scenario: a) engagement geometry, b) PNG impact angle zone, and c) orientation trajectory.

$$\alpha_{mf} \in \left[\alpha^*_{mf} \quad \theta_0 + \sin^{-1}(-\beta \sin\theta_0)\right], \qquad N \geq 3 \tag{12}$$

Note that $N \to \infty$ is the tightest turn possible, and a smaller value of N (that is, $N = 3$) will result in a curved trajectory, intercepting the surface target with an angle of less than $\alpha_{mf} < \theta_0 + \sin^{-1}(-\beta \sin\theta_0)$. The achievable impact angles using PN guidance (with $\theta_0 = 0$) lie in the shaded region, as shown in Fig. 1b. Impact angles with $N < 3$, satisfying Eq. (5), cannot be achieved by PN guidance against a nonstationary nonmaneuvering target, because the lateral acceleration demand may go to infinity near interception.

III. Orientation Guidance

We consider $\alpha_{mf} \in [-\pi \quad 0]$ as the desired set of impact angles against a surface moving target. As shown in the previous section, the classical PNG ($N \geq 3$) does not cover this desired range of impact angles completely. For all impact angles outside the range given by Eq. (12), we propose an orientation guidance for the initial phase of the interceptor flight. The interceptor follows the orientation trajectory (as shown in Fig. 1c) until the value of N, satisfying the following relation, becomes equal to three:

$$N = (\alpha_{mf} - \alpha_m) \Big/ \left(\tan^{-1}\left[\frac{\sin\alpha_{mf} - \beta\sin\alpha_t}{\cos\alpha_{mf} - \beta\cos\alpha_t}\right] - \theta\right) \tag{13}$$

After which, the interceptor follows PN guidance with $N = 3$. As shown in Fig. 1c, the achievable impact angle band, using PN guidance at the time of firing the interceptor, is the shaded region 1. As the interceptor reaches point 2 on the orientation trajectory, the achievable band shifts to the shaded region 2. The purpose of the orientation guidance is to eventually take the interceptor to point 3, in Fig. 1c. Point 3 on the orientation trajectory is chosen such that, if the interceptor switches to $N = 3$, the resulting impact angle $\alpha_{mf} = -\pi$. Thus, the union of all the shaded impact angle regions formed by tracing the orientation trajectory is $\alpha_{mf} \in [0, -\pi]$. This result is proved in Sec. III.B.

A. Orientation Guidance Command

For orientation guidance, we propose the PN guidance law:

$$\dot{\alpha}_m = N\dot{\theta} \tag{14}$$

The orientation trajectory takes the interceptor from points 1 to 3, as shown in Fig. 1c. At point 3, if the interceptor switches to PN guidance with $N = 3$, the resulting impact angle is $\alpha_{mf} = -\pi$. Using Eq. (4), with $\alpha_t = 0$ and $\alpha_{mf} = -\pi$, we have $\theta_f = -\pi$. Substituting the preceding values in Eq. (13), we have at point 3

$$\frac{-\pi - \alpha_m}{-\pi - \theta} = 3 \Rightarrow \alpha_m = 2\pi + 3\theta \tag{15}$$

We choose $\alpha_m = 0$ and $\theta = -2\pi/3$, satisfying Eq. (15) for the terminal point on the orientation trajectory. To execute the orientation maneuver, that is, to take the interceptor from $(\theta, \alpha_m) = (0, \alpha_{m0})$ (see point 1 in Fig. 1c) to $(\theta, \alpha_m) = (-2\pi/3, 0)$ (see point 3 in Fig. 1c), the orientation navigation constant is derived as

$$N = \frac{\alpha_{m0} - 0}{0 - [-(2\pi/3)]} = \frac{3\alpha_{m0}}{2\pi} \tag{16}$$

Note that

$$N \in (0,\ 1.5) \qquad \alpha_{m0} \in (0,\ \pi) \tag{17}$$

Using Eqs. (14) and (16), the orientation guidance command is given by

$$a_m = \left(\frac{3\alpha_{m0}}{2\pi}\right) v_m \dot{\theta} \tag{18}$$

The orientation navigation constant is a function of α_{m0}, and the effect of the other engagement parameters like v_t is reflected in the orientation command through $\dot{\theta}$.

B. Properties of the Orientation Trajectory

Using Eq. (18), we have, on the orientation trajectory

$$\dot{\alpha}_m = \frac{a_m}{v_m} = \frac{3}{2\pi}\alpha_{m0}\dot{\theta} \tag{19}$$

Integrating with respect to time,

$$\alpha_m = \frac{3}{2\pi}\alpha_{m0}\theta + \alpha_{m0} \tag{20}$$

Equation (20) relates the interceptor heading and the line-of-sight angle on the orientation trajectory.

Proposition 1: On the orientation trajectory the line-of-sight rate $\dot{\theta} < 0$:

Proof 1: For a moving target, with $\alpha_t = 0$, we have

$$\dot{\theta} = \frac{v_t}{R}\sin(-\theta) - \frac{v_m}{R}\sin(\alpha_m - \theta) \tag{21}$$

Using Eq. (20) in Eq. (21), we have

$$\dot{\theta} = \frac{v_t}{R}\sin(-\theta)\left[1 - \frac{\sin\{\alpha_{m0} + [(3/2\pi)\alpha_{m0} - 1]\theta\}}{\beta\sin(-\theta)}\right] \tag{22}$$

On the orientation trajectory, that is, $\theta \in [0, \ -2\pi/3]$, we have

$$\sin\left[\alpha_{m0} + \left(\frac{3}{2\pi}\alpha_{m0} - 1\right)\theta\right] \in \left[\sin\alpha_{m0} \quad \sin\left(\tfrac{2\pi}{3}\right)\right] \tag{23}$$

$$\sin(-\theta) \in \left[0 \quad \sin(2\pi/3)\right] \tag{24}$$

Using Eqs. (23) and (24) with $\alpha_{m0} \in (0, \ \pi)$, we have

$$\frac{\sin\{\alpha_{m0} + [(3/2\pi)\alpha_{m0} - 1]\theta\}}{\sin(-\theta)} \geq 1 \tag{25}$$

for all

$$\theta \in \left[-\frac{2\pi}{3}, \ 0\right]$$

From Eq. (25) with $\beta \leq \frac{1}{2}$, we have

$$\frac{\sin\{\alpha_{m0} + [(3/2\pi)\alpha_{m0} - 1]\theta\}}{\beta\sin(-\theta)} > 1 \tag{26}$$

for all

$$\theta \in \left[-\frac{2\pi}{3}, \ 0\right]$$

Using Eq. (26) in Eq. (22), we have

$$\dot{\theta} < 0 \tag{27}$$

□

Proposition 2: On the orientation trajectory:

$$\bigcup_{\theta[-2\pi/3 \quad 0]} [\alpha^*_{mf} \quad \theta + \sin^{-1}(-\beta\sin\theta)] = [-\pi \quad 0]$$

Proof 2: Let

$$q_1 = \frac{\alpha^*_{mf}}{3} \tag{28}$$

$$q_2 = \theta + \sin^{-1}(-\beta\sin\theta) \tag{29}$$

Using Eq. (10), and substituting $\alpha^*_m = 3q_1$ into it, we have on the orientation trajectory

$$\frac{\sin(3q_1)}{[\cos(3q_1) - \beta]} = \tan\left(\frac{3q_1 - \alpha_m}{3} + \theta\right) \tag{30}$$

$$\Rightarrow \frac{\sin 2q_1\cos q_1 + \cos 2q_1\sin q_1}{\cos 2q_1\cos q_1 - \sin 2q_1\sin q_1 - \beta} = \tan(q_1 + a) \tag{31}$$

where

$$a = \theta - \frac{\alpha}{3} \tag{32}$$

Simplifying Eq. (31), we have

$$\frac{\sin 2q_1\cos q_1 + \cos 2q_1\sin q_1}{\cos 2q_1\cos q_1 - \sin 2q_1\sin q_1 - \beta} = \frac{\sin q_1\cos a + \cos q_1\sin a}{\cos q_1\cos a - \sin q_1\sin a} \tag{33}$$

Further simplifying, we have

$$\frac{2\sin q_1\cos^2 q_1 + 2\cos^2 q_1\sin q_1 - \sin q_1}{2\cos^3 q_1 - \cos q_1 - 2\sin^2 q_1\cos q_1 - \beta} = \frac{\sin q_1\cos a + \cos q_1\sin a}{\cos q_1\cos a - \sin q_1\sin a} \tag{34}$$

Rearranging and simplifying the terms, after cancellation, we have

$$-\beta\sin q_1\cos a - \beta\cos q_1\sin a = \sin 2q_1\cos a - \cos 2q_1\sin a \tag{35}$$

$$\Rightarrow \frac{-\beta\sin q_1 - \sin 2q_1}{-\cos 2q_1 + \beta\cos q_1} = \tan a \tag{36}$$

$$\Rightarrow \frac{\beta\sin q_1 + \sin 2q_1}{-\cos 2q_1 + \beta\cos q_1} = \tan(-a) \tag{37}$$

Substituting the value of a, using Eq. (32), into Eq. (37), we have

$$\frac{\sin 2q_1 + \beta\sin q_1}{-\cos 2q_1 + \beta\cos q_1} = \tan\left(\frac{\alpha_m}{3} - \theta\right) \tag{38}$$

Differentiating Eq. (38) with respect to θ, we have

$$\frac{(-2 + \beta^2 + \beta\cos 3q_1)}{[-\cos 2q_1 + \beta\cos q_1]^2}\frac{dq_1}{d\theta} = \sec^2\left(\frac{\alpha_m}{3} - \theta\right)\left(\frac{1}{3}\frac{d\alpha_m}{d\theta} - 1\right) \tag{39}$$

Differentiating Eq. (20) with respect to θ, we have on the orientation trajectory

$$\frac{d\alpha_m}{d\theta} = \frac{3}{2\pi}\alpha_{m0} \tag{40}$$

Using Eq. (40) in Eq. (39), we have

$$\frac{(-2 + \beta^2 + \beta\cos 3q_1)}{[-\cos 2q_1 + \beta\cos q_1]^2}\frac{dq_1}{d\theta} = \sec^2\left(\frac{\alpha_m}{3} - \theta\right)\left(\frac{\alpha_{m0}}{2\pi} - 1\right) \tag{41}$$

$$\Rightarrow \frac{\mathrm{d}q_1}{\mathrm{d}\theta} > 0 \tag{42}$$

Because

$$\frac{(-2 + \beta^2 + \beta\cos q_1)}{[-\cos 2q_1 + \beta\cos q_1]^2} < 0 \tag{43}$$

for all

$$\beta \leq \tfrac{1}{2}$$

and

$$3\sec^2\left(\frac{\alpha_m}{3} - \theta\right)\left(\frac{\alpha_{m0}}{2\pi} - 1\right) < 0 \tag{44}$$

for all

$$\alpha_{m0} \in (0, \ \pi)$$

Differentiating Eq. (29) with respect to θ, we have

$$\frac{\mathrm{d}q_2}{\mathrm{d}\theta} = \left[1 - \frac{\beta\cos\theta}{\sqrt{(\beta\cos\theta)^2 + 1 - (\beta)^2}}\right] > 0 \tag{45}$$

because $\beta \leq 1/2$. Using Eqs. (42) and (45), we have

$$\bigcup_{\theta\in[-2\pi/3 \quad 0]} \left[3q_1 \quad q_2\right] = \left[\min\{3q_1(\theta = -2\pi/3), \ q_2(\theta = -2\pi/3)\} \quad \max\{3q_1(\theta = 0), \ q_2(\theta = 0)\}\right] \tag{46}$$

At the initial point of the orientation trajectory (see point 1 in Fig. 1c) with $\theta = 0$, we have [using Eq. (29)]

$$q_2(\theta = 0) = 0 \tag{47}$$

which is the maximum possible impact angle in a surface-to-surface to engagement. Therefore, using Eq. (47), we have

$$\max[3q_1(\theta = 0),\ q_2(\theta = 0)] = 0 \tag{48}$$

At the terminal point of the orientation trajectory (see point 3 in Fig. 1c), we have $\theta = -2\pi/3$ and $\alpha_m = 0$. The values of θ and α_m at this point satisfy Eq. (30). Therefore, we have

$$3q_1(\theta = -2\pi/3) = \alpha_{mf}(\theta = -2\pi/3) = -\pi \tag{49}$$

which is the minimum possible impact angle for a surface-to-surface engagement. Using Eq. (49), we have

$$\min[3q_1(\theta = -2\pi/3),\ q_2(\theta = -2\pi/3)] = -\pi \tag{50}$$

Using Eqs. (48) and (50) in Eq. (46), we have

$$\bigcup_{\theta \in \begin{bmatrix} -2\pi/3 & 0 \end{bmatrix}} \begin{bmatrix} 3q_1 & q_2 \end{bmatrix} = \begin{bmatrix} \min\{3q_1(\theta = -2\pi/3),\ q_2(\theta = -2\pi/3)\} & \max\{3q_1(\theta = 0),\ q_2(\theta = 0)\} \end{bmatrix} = \begin{bmatrix} -\pi & 0 \end{bmatrix} \tag{51}$$

□

IV. The Proposed Guidance Law

Proposition 2 shows that for any impact angle in $[-\pi \quad 0]$, there exists a point on the orientation trajectory from which the PN guidance law with $N \geq 3$ results in the desired interception. The proposed two-stage PN guidance law follows the orientation guidance command given by Eq. (18) if the value of N, satisfying Eq. (13), is less than three until Eq. (13) is satisfied with $N = 3$. After which, $N = 3$ is used. The proposed guidance law is given as

$$a_m = N v_m \dot{\theta} \tag{52}$$

For engagement geometries with $(\alpha_{mf} - \alpha_{m0})/(\theta_f - \theta_0) \geq 3$

$$N = \frac{\alpha_{mf} - \alpha_{m0}}{\theta_f - \theta_0} \tag{53}$$

For engagement geometries with $(\alpha_{mf} - \alpha_{m0})/(\theta_f - \theta_0) \geq 3$

$$N = \begin{cases} \frac{3\alpha_{m0}}{2\pi} & \text{if } t < t_s \\ 3 & \text{if } t \geq t_s \end{cases} \tag{54}$$

where t_s is the switching time when the value of the expression $(\alpha_{mf} - \alpha_m)/(\theta_f - \theta)$ increases to a value of three.

V. Simulation Results

A. Constant Speed Interceptor

To demonstrate the basic properties of the proposed guidance law, we use a constant speed interceptor model. We consider $v_m = 300$ m/s and $v_t = 100$ m/s with $\alpha_t = 0$, the interceptor initial position $(x_{m0},\ z_{m0}) = (0,\ 0)$, and the target initial position $(x_{t0},\ z_{t0}) = (5000m,\ 0)$. Simulations are terminated for a closing range of $(R < 0.1$ m). The interceptor has a maximum lateral acceleration limit of ± 15 g.

We consider $\alpha_{m0} = 30$ deg and $\alpha_{mf} = -90$ deg for the simulation. The corresponding value of $(\alpha_{mf} - \alpha_{m0})/(\theta_f - \theta_0) = 1.1066$, which is outside the capturable impact angle set [see Eq. (12)] for the classical PNG ($N \geq 3$). Solid lines in Figs. 2a and 2b show the interceptor trajectory and lateral acceleration profile, respectively, for the proposed guidance law. The engagement results in the successful interception of the target with a negligible impact angle error of 0.034 deg. The variation in N is plotted in Fig. 2c. The interceptor follows the orientation trajectory in the first phase of the guidance with $N = 3/(2\pi)\alpha_{m0} = 3/(2\pi)\pi/6 = 0.25$. With this smaller value of N, the orientation lateral acceleration is also lower (see Fig. 2b). On the orientation trajectory, the value of $(\alpha_{mf} - \alpha_m)/(\theta_f - \theta)$ increases from the initial value of 1.1066 (dashed lines, see Fig. 2c). The interceptor departs from the orientation trajectory as $(\alpha_{mf} - \alpha_m)/(\theta_f - \theta)$ increases to three and switches to $N = 3$. Switching to a higher value of N results in a sudden increase in lateral acceleration (see Fig. 2b). After switching to $N = 3$, the lateral acceleration reduces to zero near interception. As $(\alpha_{mf} - \alpha_m) \to 0$ and $(\theta_f - \theta) \to 0$ near interception, the value of $(\alpha_{mf} - \alpha_m)/(\theta_f - \theta) \to 1$ (see Fig. 2c). Dashed lines in Figs. 2a and 2b represent the corresponding results for classical PNG with $N = 1.1066$. The terminal lateral acceleration demand for PNG increases rapidly as Eq. (6) is violated and results in an impact angle error of 35.45 deg. We compare the capturability of the proposed guidance law with the existing trajectory shaping guidance law [11] that, by linearization, can also be simplified to obtain the optimal impact angle constrained guidance law [5]. The trajectory shaping law is given as

$$a_m = 4V_c\dot{\theta} + 2V_c\frac{(\theta_f - \theta)}{t_{\text{go}}} \tag{55}$$

where V_c is the closing speed and t_{go} is the time to go. We vary the desired impact angle α_{mf} and compare the performance in terms of the impact angle error. The comparative results are shown in Fig. 2d. The proposed guidance law captures all impact angles $\alpha_{mf} \in [-\pi,\ 0]$ for which, as the trajectory shaping guidance law breaks down, nears head-on kind of desired terminal geometries.

B. Realistic Interceptor

To validate the applicability of the proposed guidance law in realistic engagement scenarios, we carry out simulations with a realistic interceptor model. The detailed model with vehicle and aerodynamic properties is described in Kee et al. [12] and is borrowed here. All simulations are terminated for a closing distance of $R < 0.5$ m. We consider a ± 20 g limit on the maximum lateral acceleration. As the guidance loop is closed after the first boost phase is over, the orientation command derived from Eq. (16) is modified (for realistic engagements) as

$$N = \frac{(-0 - \alpha_{m\text{GLC}})}{[-2\pi/3) - \theta_{\text{GLC}})]} = \frac{\alpha_{m\text{GLC}}}{[(2\pi/3) + \theta_{\text{GLC}}]} \tag{56}$$

where $\alpha_{m\text{glc}}$ and θ_{glc} are the interceptor heading and line-of-sight angle, respectively, at the time of the guidance loop closure (GLC). From Eq. (4), we see that, for a predefined α_{mf}, the value of θ_f varies with THE interceptor speed. Thus, for realistic engagements, the value of $(\alpha_{mf} - \alpha_m)/(\theta_f - \theta)$ may deviate from the switching value with a variation in the interceptor speed and may fall below the minimum allowable limit of $2(1 + \beta)$. We include the minimum allowable limit on the navigation constant in the terminal phase for

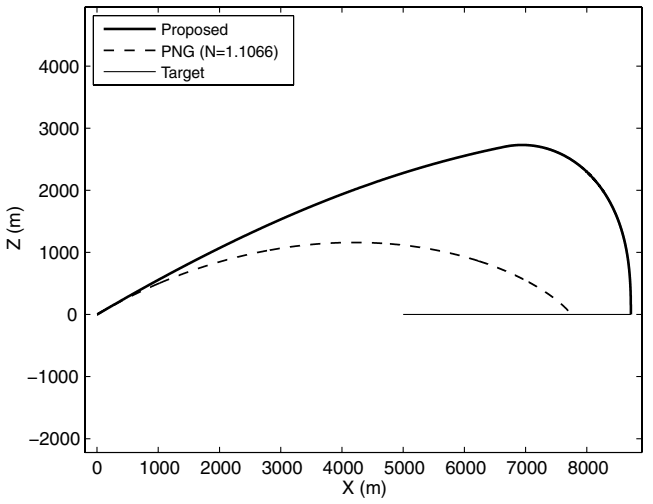

a) Trajectories

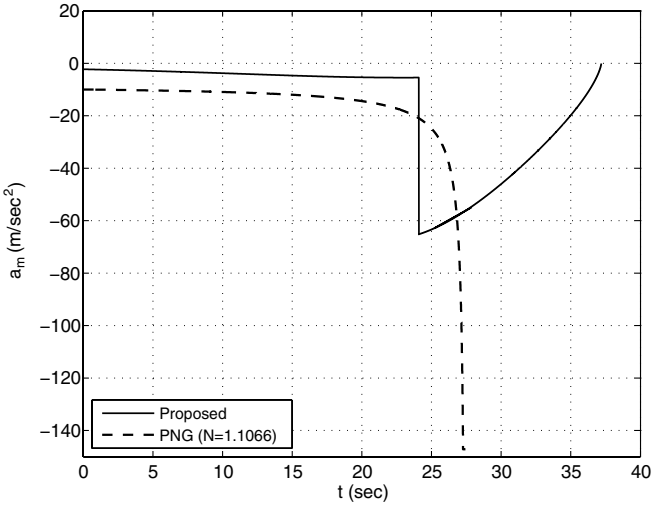

b) Lateral acceleration profiles

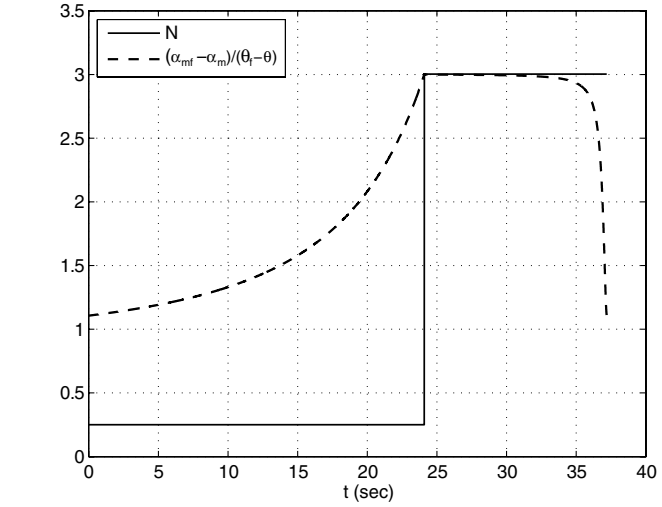

c) N, $\dfrac{\alpha_{mf}-\alpha_m}{\theta_f-\theta}$ vs time

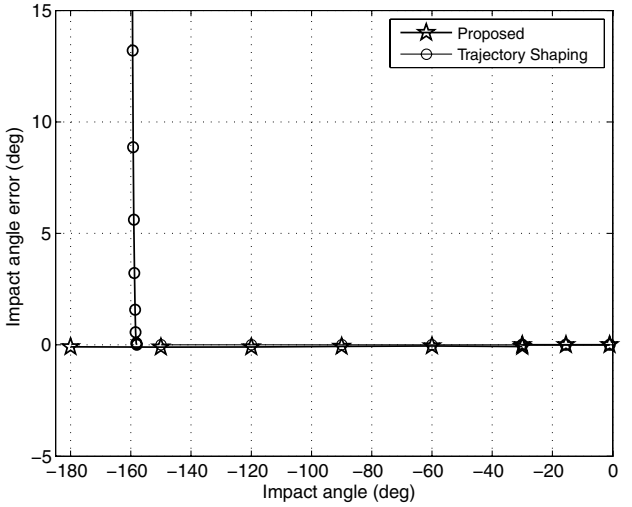

d) Capturability comparison

Fig. 2 Results for case 1: constant speed interceptor model.

realistic engagements. The modified guidance law, with the gravity compensation, is gives as follows:

$$a_m = Nv_m\dot{\theta} + g\cos\alpha_m \tag{57}$$

For engagement geometries with $(\alpha_{mf} - \alpha_{m0})/(\theta_f - \theta_0) \geq 3$,

$$N = \frac{\alpha_{mf} - \alpha_m}{\theta_f - \theta} \tag{58}$$

For engagement geometries with $(\alpha_{mf} - \alpha_{m0})/(\theta_f - \theta_0) < 3$,

$$N = \begin{cases} \dfrac{\alpha_{m\text{glc}}}{\dfrac{2\pi}{(\frac{}{3}+\theta_{\text{glc}})}} & \text{if } \dfrac{\alpha_{mf}-\alpha_m}{\theta_f-\theta} < 3,\ t < t_s \\ \dfrac{\alpha_{mf}-\alpha_m}{\theta_f-\theta} & \text{if } \dfrac{\alpha_{mf}-\alpha_m}{\theta_f-\theta} > 2(1+\beta),\ t > t_s \\ 2(1+\beta) & \text{if } \dfrac{\alpha_{mf}-\alpha_m}{\theta_f-\theta} \leq 2(1+\beta),\ t > t_s \end{cases} \tag{59}$$

where t_s is the switching time, which is defined as the time when the condition $(\alpha_{mf} - \alpha_m)/(\theta_f - \theta) = 3$ is satisfied first and the interceptor leaves the orientation trajectory. Note that the navigation constants in Eqs. (58) and (59) are no longer constants and are updated at every guidance cycle.

We consider the desired impact angles to be outside the capture region of the classical PN guidance law ($N \geq 3$) with $v_t = 50$ m/s, $(x_{m0}, z_{m0}) = (0, 0)$ and $(x_{t0}, z_{t0}) = (5000m, 0)$. The interceptor is launched with $\alpha_{m0} = 30$ deg. The desired impact angles are $\alpha_{mf} = -45, -90, -135$, and -180 deg. The trajectories (plotted in Fig. 3a) show successful interception of the target. The interceptor flies unguided for the first boost phase (1.5 s) and then follows the orientation command (see Fig. 3b) before switching to attain the desired impact angle. The corresponding impact angle errors are less than 1 deg. The proposed guidance scheme is derived using the nonmaneuvering target model. However, Eq. (57) is a feedback guidance law that can be used against maneuvering targets. Next, we consider $\alpha_{mf} = -10, -90, -180$ deg and simulate engagements with different target step acceleration a_t levels. The impact angle errors are plotted in Fig. 3c. Impact angle errors for $\alpha_{mf} = -90$, 180 deg are less than 2 and 4 deg, respectively, for target accelerations up to 4 m/s^2. For $\alpha_{mf} = -10$ deg, the target closes to the interceptor early, leading to lateral acceleration saturation, resulting in higher impact angle errors. To study the robustness of the proposed guidance law, we simulate trajectories for the values of the first-order autopilot lag time constant τ, up to 0.3 s. The results, as plotted in Fig. 3d, show less than a 2 deg error in impact angle for $\alpha_{mf} = -90$ and $\alpha_{mf} = -180$ deg. For $\alpha_{mf} = -10$ deg, the lateral acceleration saturation causes an error of around 2.4 deg (even with

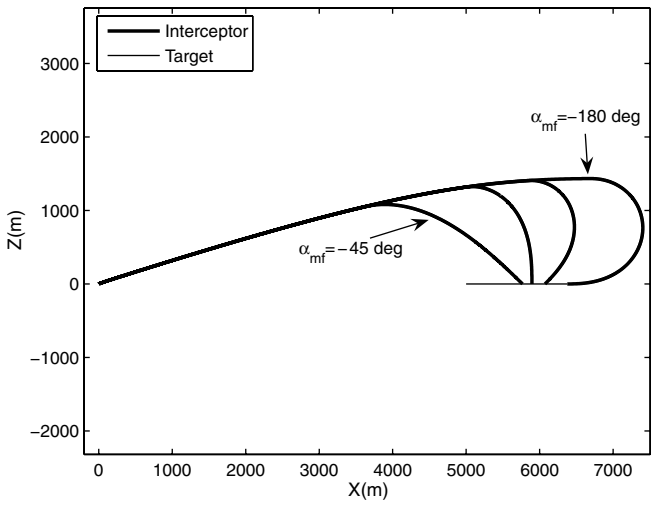

a) Trajectories

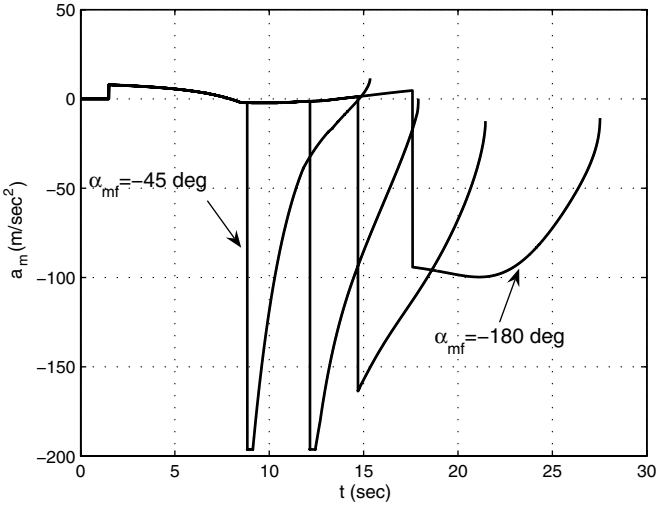

b) Lateral accelaration

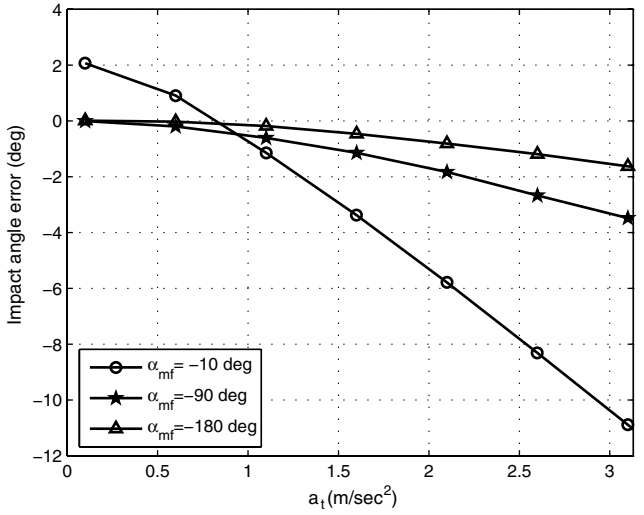

c) Impact angle error vs a_t

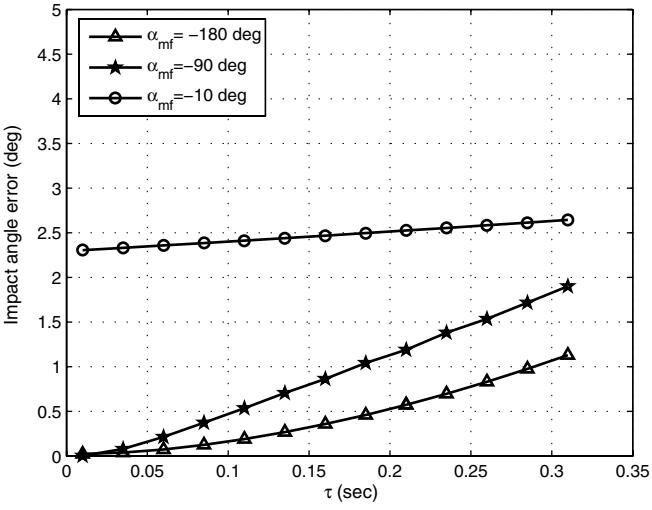

d) Impact angle error vs τ

Fig. 3 Results for case 2: realistic interceptor model.

no delays), and the error increases by 0.2 deg for the considered range of τ.

VI. Conclusions

A two-stage PNG-based guidance law for impact angle constrained interception of nonstationary nonmaneuvering targets in a surface-to-surface engagement scenario is presented. The orientation guidance (PNG with a lower N) facilitates the interceptor to switch to $N = 3$ and achieve any desired impact angle for surface-to-surface applications. The feedback implementable form of the guidance law is also presented for realistic engagements. Simulation results show successful achievement of all impact angles for constant speed and realistic interceptor models. Robustness of the proposed guidance law is verified by realistic simulations with first-order autopilot lags. Proportional navigation provides the inherent simplicity, robustness, and implementation feasibility to the proposed guidance scheme. The impact angle performance is limited by the choice of impact angle in the maneuvering target scenario.

References

[1] Kim, M., and Grider, K. V., "Terminal Guidance for Impact Attitude Angle Constrained Flight Trajectories," *IEEE Transactions on Aerospace and Electronic Systems*, Vol. 9, No. 6, Dec. 1973, pp. 852–859.
doi:10.1109/TAES.1973.309659

[2] York, R. J., and Pastrick, H. L., "Optimal Terminal Guidance with Constraints at Final Time," *Journal of Spacecraft and Rockets*, 14, June 1977, pp. 381–382.
doi:10.2514/3.57212

[3] Kim, B. S., Lee, J. G., and Han, H. S., "Biased PNG Law for Impact with Angular Constraint," *IEEE Transactions on Aerospace and Electronic Systems*, Vol. 34, No. 1, Jan. 1998, pp. 277–288.
doi:10.1109/7.640285

[4] Ohlmeyer, E. J., and Phillips, C. A., "Generalized Vector Explicit Guidance," *Journal of Guidance, Control, and Dynamics*, Vol. 29, No. 2, March–April 2006, pp. 261–268.
doi:10.2514/1.14956

[5] Ryoo, C. K., Cho, H., and Tahk, M. J., "Optimal Guidance Laws with Terminal Impact Angle Constraint," *Journal of Guidance, Control, and Dynamics*, Vol. 28, No. 4, July–Aug. 2005, pp. 724–732.
doi:10.2514/1.8392

[6] Shafferman, V., and Shima, T., "Linear Quadratic Differential Games Guidance Law for Imposing a Terminal Intercept Angle," *Journal of Guidance, Control, and Dynamics*, Vol. 31, No. 5, Sept.–Oct. 2008, pp. 1400–1412.
doi:10.2514/1.32836

[7] Ratnoo, A., and Ghose, D., "State Dependent Riccati Equation Based Guidance Law for Impact Angle Constrained Trajectories," *Journal of Guidance, Control, and Dynamics*, Vol. 32, No. 1, Jan.–Feb. 2009, pp. 320–326.
doi:10.2514/1.37876

[8] Lu, P., Doman, D. B., and Schierman, J. D., "Adaptive Terminal Guidance for Hypervelocity Impact in Specified Direction," *Journal of Guidance, Control, and Dynamics*, Vol. 29, No. 2, March–April 2006,

pp. 269–278.
doi:10.2514/1.14367

[9] Ratnoo, A., and Ghose, D., "Impact Angle Constrained Interception of Stationary Targets," *Journal of Guidance, Control, and Dynamics*, Vol. 31, No. 6, Nov.–Dec. 2008, pp. 1816–1821.
doi:10.2514/1.37864

[10] Guelman, M., "A Qualitative Study of Proportional Navigation," *IEEE Transactions on Aerospace and Electronic Systems*, Vol. 7, July 1971, pp. 637–643.
doi:10.1109/TAES.1971.310406

[11] Zarchan, P., *Tactical and Strategic Missile Guidance*, 4th ed., Vol. 199, AIAA, Reston, VA, 2002, pp. 541–568.

[12] Kee, P. E., Dong, L., and Siong, C. J., "Near Optimal Midcourse Guidance Law for Flight Vehicle," 36th AIAA Aerospace Sciences Meeting and Exhibit, AIAA 1998-583, 12–15 Jan. 1998.